Analyzing the growth of $In_xGa_{1-x}N$/GaN superlattices in self-induced GaN nanowires by x-ray diffraction

M. Wölz,[a] V. M. Kaganer, O. Brandt, L. Geelhaar, and H. Riechert
Paul-Drude-Institut für Festkörperelektronik, Hausvogteiplatz 5–7, 10117 Berlin, Germany

(Received 11 February 2011; accepted 7 June 2011; published online 28 June 2011)

Self-induced GaN nanowires are grown by plasma-assisted molecular beam epitaxy, with $In_xGa_{1-x}N$ quantum wells inserted to form an axial superlattice. From the $\omega-2\theta$ scans of a laboratory x-ray diffraction experiment, we obtain the superlattice period, the thickness of the quantum wells, and the In content in this layer. The axial growth rate of the $In_xGa_{1-x}N$ quantum wells is significantly enhanced, which we attribute to increased Ga diffusion along the nanowire sidewalls in the presence of In. © *2011 American Institute of Physics*. [doi:10.1063/1.3604810]

In semiconductor nanowires (NWs) strain induced by lattice-mismatch can elastically relax at the free sidewalls.[1] For light emitting diodes (LEDs) based on nitrides, NW heterostructures may thus help to overcome efficiency limitations related to defects from plastic strain relaxation and pave a path to using cost-effective Si substrates. A particularly attractive approach to the synthesis of such NWs is the self-induced growth by plasma-assisted molecular beam epitaxy (MBE) which does not require any foreign collector material and results in GaN of outstanding quality.[2] In this way, GaN nano LEDs with axial $In_xGa_{1-x}N$/GaN NW heterostructures have been fabricated by several groups.[3–8] Obviously, control over the emission wavelength requires the predictable growth of the In-containing active region. Very little is known, however, about the underlying growth mechanisms.[9,10]

The standard technique to characterize layer thicknesses and compositions in conventional planar superlattices is high-resolution x-ray diffraction (XRD). With respect to superlattices in bottom-up grown NWs, synchrotron x-ray experiments have been carried out to investigate crystallographic phases as well as strain.[11,12] However, we are not aware of any attempts to extract the structural parameters of such superlattices from laboratory experiments. As a matter of fact, for such samples, the interpretation of XRD measurements is expected to be more complex than for planar superlattices. In order to obtain sufficient diffracted intensity with a laboratory x-ray source, a large ensemble of NWs has to be probed. On such a sample, there is invariably a significant spread in the NW length, the vertical position of the superlattice above the substrate, the layer thicknesses and composition in the superlattice, and in the orientation of the NWs with respect to the substrate. As a consequence, the amount of material contributing to constructive interference is very low. Moreover, the small diameter of the NWs results in increased peak width in reciprocal space. All of these effects lead to significant peak broadening. Nevertheless, we show here that the main structural characteristics of $In_xGa_{1-x}N$/GaN NW superlattices can be determined from the diffraction pattern. By comparison of the x-ray results with the growth parameters, we deduce a surprisingly enhanced axial growth rate of the $In_xGa_{1-x}N$ quantum wells in the NWs.

[a]Electronic mail: woelz@pdi-berlin.de.

Self-induced GaN NWs were grown on Si(111) by MBE. The fluxes from the N plasma source and the Ga and In effusion cells were calibrated in equivalent planar GaN and InN growth rates. Prior to growth, the native Si oxide was removed *in situ* by depositing 100 monolayers of liquid Ga and desorbing it again by raising the temperature until the Si(111) 7×7 reconstruction appeared in reflection high-energy electron diffraction. After a fixed nitridation time, GaN NWs were grown at 770 °C with fluxes of 4 nm/min Ga and 20 nm/min N. After 1 h of growth, the metal flux was interrupted and the substrate temperature brought to 585 °C for the growth of the active region. Three samples with superlattices consisting of six pairs of GaN barriers and $In_xGa_{1-x}N$ quantum wells were grown with the parameters given in Table I. The barrier thickness was varied by doubling the barrier growth time from one sample to the next, while keeping all other parameters constant. The resulting superlattice is discernible in the scanning electron micrograph shown in Fig. 1. The positions of the quantum wells in the NW tips are assigned to the areas of slightly increased brightness.

X-ray measurements were carried out with $CuK\alpha_1$ radiation using a Panalytical X'Pert system with Ge(220) hybrid monochromator and Ge(220) analyzer crystal. Symmetric Bragg $\omega-2\theta$ scans across the GaN(0002) reflection are shown in Fig. 2. Satellite peaks are clearly visible, but their intensity is only slightly higher than the background. In contrast, planar $In_xGa_{1-x}N$/GaN superlattices typically used for LED structures exhibit a signal-to-noise ratio of two orders

TABLE I. $In_xGa_{1-x}N$/GaN NW superlattice samples grown with different GaN barrier growth times. The Ga flux during GaN barrier growth was $\Phi_{Ga,barrier}=4.0$ nm/min. The $In_xGa_{1-x}N$ well growth parameters were kept constant at $t_{well}=0.9$ min, $\Phi_{In}=1.7$ nm/min, and $\Phi_{Ga,well}=0.8$ nm/min.

	Growth	Parameters determined from: Peak positions		Parameters determined from: Simulations				
Sample	$t_{barrier}$ (min)	d_{SL} (nm)	x_{avg} (%)	d_{SL} (nm)	x_{avg} (%)	d_{well} (nm)	x_{well} (%)	σ_d (nm)
(a)	1.58	10.8	9.2	9.9	8.1	2.7	30	1.6
(b)	3.36	19.3	5.0	19.0	5.0	3.8	25	2.4
(c)	6.88	33.0	2.9	33.0	3.0	3.2	31	3.4

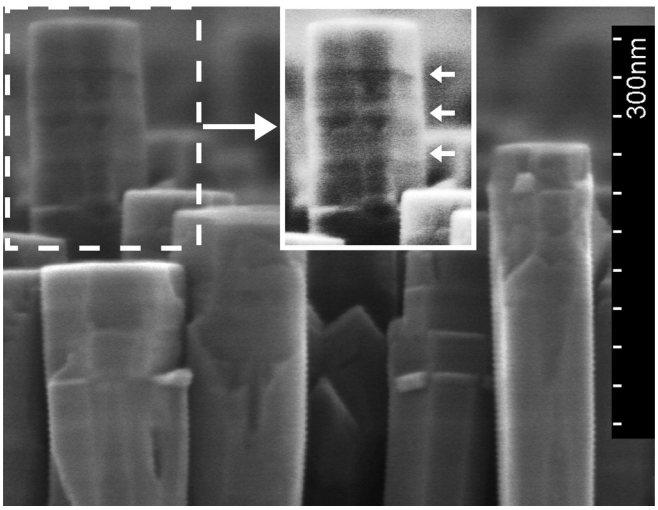

FIG. 1. Scanning electron micrograph of GaN nanowire tips with an inserted $In_xGa_{1-x}N$/GaN heterostructure with a superlattice period of 33 nm [sample (c)]. The inset shows the same NW with enhanced contrast.

of magnitude or more. The interpretation of our scans is not as straightforward as for planar layers, because the broad satellite peaks with low intensity could correspond either to thickness fringes from the $In_xGa_{1-x}N$/GaN superlattice or to individual $In_xGa_{1-x}N$ layers with varying composition. However, the consideration of the entire series of samples shows that longer barrier growth time leads to more closely spaced peaks. The samples were designed such that the quantum wells can be assumed to be identical for all the samples.

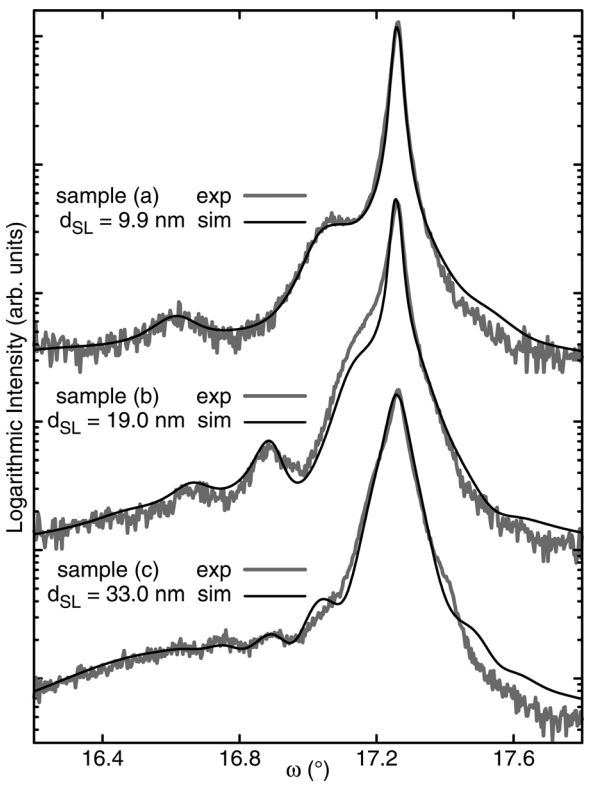

FIG. 2. XRD $\omega-2\theta$ scans (gray lines) across the GaN(0002) reflection of $In_xGa_{1-x}N$/GaN NW superlattices from samples (a), (b), and (c) with different barrier growth times. The simulations (black lines) take into account the superlattice peak broadening due to fluctuations of the layer thicknesses. The simulated superlattice period d_{SL} is given in the graphs.

Therefore, the broad peaks are diffraction satellites due to the periodic superlattice.

On the basis of this interpretation, we can extract structural information from the XRD scans. The positions ω_n of the satellites are related to the superlattice period d_{SL} via Bragg's law, $d_{SL} = \lambda/[2(\sin\omega_n - \sin\omega_{n-1})]$, where λ is the wavelength of the x-rays. The resulting values for d_{SL} are given in Table I. d_{SL} is the sum of the barrier and quantum well thicknesses $d_{barrier}$ and d_{well}. Whereas these cannot be directly inferred from the Bragg interpretation, information can be extracted by comparing the three samples under investigation. They were grown in the same way, and the only difference is the growth time for the GaN barriers between the wells. Assuming an abrupt change between well and barrier growth, the superlattice period as a function of barrier growth time $t_{barrier}$ is

$$d_{SL} = d_{barrier} + d_{well} = R_{barrier} t_{barrier} + d_{well}, \qquad (1)$$

where $R_{barrier}$ is the GaN NW barrier growth rate. In Fig. 3, the superlattice periods obtained from the x-ray data are plotted as a function of $t_{barrier}$ for the three samples. The linear relationship of Eq. (1) is confirmed and the barrier growth rate is determined to be $R_{barrier} = 4.1 \pm 0.2$ nm/min. The GaN NW growth rate is, therefore, comparable to the calibrated Ga flux $\Phi_{Ga,barrier} = 4.0$ nm/min, as has been shown for self-induced GaN NWs before.[13,14]

The plot in Fig. 3 contains even more information. By extrapolating the straight line through the data points to $t_{barrier} = 0$, the contribution of the barrier is subtracted from d_{SL} and the absolute quantum well thickness is obtained from the axis intercept as $d_{well} = 4.7 \pm 1.0$ nm. This value needs to be taken with some caution, since we assumed an abrupt change from $In_xGa_{1-x}N$ to GaN growth when the In shutter is closed. The activation energy for InN dissociation is lower than for In evaporation from droplets,[15] and In segregation during quantum well growth is known for planar layers.[16] The same might be the case for NWs, and d_{well} from Eq. (1) can, therefore, be considered as a lower boundary for the well thickness.

The superlattice composition can be obtained via Bragg's law as follows. The zeroth order superlattice peak position ω_0 gives the average lattice constant in c-direction of the superlattice: $c_{avg} = 2d_{0002} = \lambda/\sin\omega_0$. Assuming that

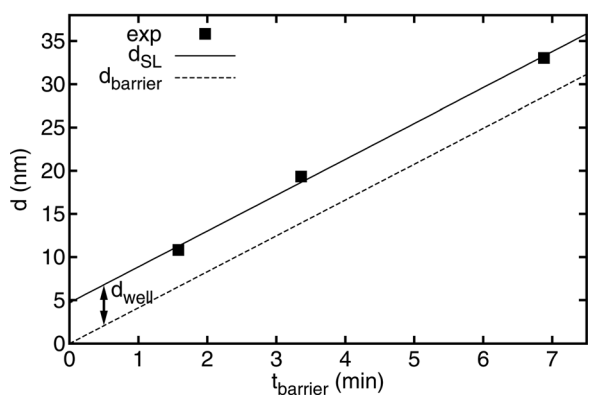

FIG. 3. Superlattice periods d_{SL} experimentally obtained from the distances between satellite peaks. d_{SL} is the sum of the barrier and well thicknesses $d_{barrier}$ and d_{well} and depends linearly on the barrier growth time $t_{barrier}$.

the $In_xGa_{1-x}N$ lattice parameter in c-direction follows Vegard's law and is increased due to elastic strain, the average composition x_{avg} is related to c_{avg} as

$$\frac{c_{avg} - c_{GaN}}{c_{InN} - c_{GaN}} = x_{avg}\left(\frac{1+v}{1-v} - \beta\right), \quad (2)$$

where v is the Poisson ratio whose value was taken as 0.23.[17] For NWs with diameter much larger than the total thickness of the heterostructure, lateral strain relief does not occur and $\beta = 0$. Heterostructures in nanowires are known, however, to relax laterally.[12,18] Ignoring the elastic constraint imposed by the GaN NW base, we obtain $\beta = [2v/(1-v)]d_{well}/d_{SL}$ corresponding to full lateral and vertical elastic relaxation. The values of x_{avg} are given in Table I for the latter case. The values for the limiting cases differ by no more than 20% for sample (a) which has the largest β.

To obtain the quantum well composition x_{well}, we can consider the product $d_{SL}x_{avg}$ which is the total amount of In incorporated into each superlattice period. This must be conserved regardless of the achieved quantum well thickness, and therefore

$$d_{well}x_{well} = d_{SL}x_{avg}. \quad (3)$$

Taking the data from Table I, the average over all samples is 0.98 ± 0.01 nm of equivalent InN layer thickness. The small standard deviation indicates that the quantum wells in the three samples are indeed very similar.

The standard procedure for the analysis of x-ray diffraction data is the comparison to simulations in the framework of kinematical or dynamical diffraction theory. However, algorithms developed for planar layers cannot be directly applied to NW data, as discussed in the introduction. In order to overcome this difficulty, we calculated the whole diffraction pattern in the kinematical approximation from the superlattice as a sum of intensities from individual NWs possessing different thicknesses of the barriers and wells.[19] The layer thicknesses were considered as independent Gaussian random variables. Input parameters for the calculation are the relative vertical misfit between the barrier and well layers, the barrier and the well thicknesses, and the standard deviations σ_d of the thickness distributions. Strain at the substrate interface and its successive relaxation in the base layer toward the active region was taken into account to accurately model the GaN(0002) peak broadening. The simulated curves in Fig. 2 were obtained with the parameters given in Table I. The simulation of the diffraction profiles yields the well thickness d_{well} and the In content x_{well} for each sample separately. Averaging over all samples, we find $d_{well} \approx 3.2$ nm and an In content in the well of about 28%. Fluctuations of the thicknesses of the individual layers are found to be rather large, $\sigma_d \approx 2.5$ nm. The average well thickness obtained from the simulation of the diffraction peaks is somewhat smaller than the one obtained from the axis intercept in Fig. 3, but agrees with it within the experimental error. Hence, we have shown that the structural parameters of NW superlattices can be determined from XRD data in two independent ways. The agreement between the two methods also strongly suggests an abrupt change from $In_xGa_{1-x}N$ to GaN growth. In other words, In incorporation after closing the In shutter is not significant.

Now, we use the structural information extracted from the XRD data to shed light on growth mechanisms. We determine $R_{well} = d_{well}/t_{well} = 5.2$ nm/min from the analysis of the Bragg peak positions independently of the simulation. Let us now compare this value with the quantum well growth rate that follows from the fluxes calibrated for the growth of planar layers. This latter quantity is a product of the calibrated Ga flux $\Phi_{Ga,well} = 0.8$ nm/min and the additional contribution from the In source, which gives a factor $(1 + x_{well})$. Hence, the quantum well growth rate expected from the calibrated Ga flux can be estimated as $R_{well,cal} = \Phi_{Ga,well}(1 + x_{well}) = 1.0$ nm/min. Obviously, the actual $In_xGa_{1-x}N$ NW quantum well growth rate is much higher than the amount of supplied material implies.

In order to resolve this discrepancy, we have to take into account that the growth of self-induced GaN NWs is fed both from the impinging fluxes and the diffusion of Ga along the NW sidewalls to the tip.[13,14,20] Hence, the increase in NW growth rate for the quantum wells necessitates higher diffusion flux of Ga in the presence of In. It is already known that during NW nucleation In enhances the diffusivity of Ga atoms on the substrate, leading to the suppression of rough 2D layer growth.[21] In our experiments, In was supplied only after 400 nm long GaN NWs were grown, and thus the substrate surface was shadowed to a high degree. Therefore, we conclude that In is an effective surfactant which enhances the diffusion of Ga atoms along the M-plane sidewalls of the NWs.

This drastic increase in growth rate has consequences for the controlled growth of $In_xGa_{1-x}N$/GaN NW heterostructures. The increased Ga incorporation rate has to be taken into account both for the well thickness and the In content. This result is of vital importance for the rational growth of GaN nano LEDs and the development of a comprehensive growth model for $In_xGa_{1-x}N$ quantum wells in self-induced NWs.

We are grateful to C. Herrmann, G. Jaschke, and H.-P. Schönherr for their dedicated maintenance of the MBE system and to A.-K. Bluhm for the scanning electron micrographs. This work has been partly funded by the German government BMBF project MONALISA (Contract No. 01BL0810).

[1] M. T. Björk *et al.*, Appl. Phys. Lett. **80**, 1058 (2002).
[2] C. Chèze *et al.*, Nano Res. **3**, 528 (2010).
[3] A. Kikuchi *et al.*, Jpn. J. Appl. Phys. **43**, L1524 (2004).
[4] A.-L. Bavencove *et al.*, Phys. Status Solidi A **207**, 1425 (2010).
[5] W. Guo *et al.*, Nano Lett. **10**, 3355 (2010).
[6] R. Armitage and K. Tsubaki, Nano Technol. **21**, 195202 (2010).
[7] H. W. Lin *et al.*, Appl. Phys. Lett. **97**, 073101 (2010).
[8] Y.-L. Chang *et al.*, Appl. Phys. Lett. **96**, 013106 (2010).
[9] H. Sekiguchi *et al.*, Appl. Phys. Lett. **96**, 231104 (2010).
[10] G. Tourbot *et al.*, Nano Technol. **22**, 075601 (2011).
[11] J. Eymery *et al.*, Nano Lett. **7**, 2596 (2007).
[12] M. Hanke *et al.*, Phys. Rev. B **75**, 161303 (2007).
[13] C. Chèze *et al.*, Appl. Phys. Lett. **97**, 153105 (2010).
[14] S. Fernandez-Garrido *et al.*, J. Appl. Phys. **106**, 126102 (2009).
[15] C. S. Gallinat *et al.*, J. Appl. Phys. **102**, 064907 (2007).
[16] P. Waltereit *et al.*, Phys. Rev. B **66**, 165322 (2002).
[17] H. H. Lee *et al.*, Appl. Phys. Lett. **81**, 5120 (2002).
[18] S. Keller *et al.*, J. Appl. Phys. **100**, 054314 (2006).
[19] V. M. Kaganer *et al.*, X-ray diffraction profiles from axial nanowire heterostructures, Phys. Rev. B (in press).
[20] R. K. Debnath *et al.*, Appl. Phys. Lett. **90**, 123117 (2007).
[21] O. Landre *et al.*, Appl. Phys. Lett. **93**, 183109 (2008).